18TH WORLD CONFERENCE ON EARTHQUAKE ENGINEERING
WCEE2024
MILAN

MILAN, ITALY
30TH JUNE - 5TH JULY 2024
www.wcee2024.it

SEISMIC FRAGILITY ASSESSMENT OF SPHERICAL PRESSURE VESSELS: THE EFFECT OF FILL RATIO VARIABILITY

N. D. Karaferis[1], V. E. Melissianos[2] & D. Vamvatsikos[2]

[1] School of Civil Engineering, National Technical University of Athens, Greece, nkaraferis@mail.ntua.gr

[2] School of Civil Engineering, National Technical University of Athens, Greece

Abstract: *Fragility curves are a seismic risk modeler's bread and butter, relaying the probability of reaching or exceeding each limit state of interest given the ground motion intensity. Yet, as they convey essential information, they also hide assumptions, especially when used to characterize a group of similar or even seemingly identical structures. Chief among them is the concept that the dynamic properties of such structures are invariable and uncorrelated. However, the latter does not necessarily apply to groups of adjacent "identical" spherical pressure vessels, used for storing gaseous products in industrial facilities. The quantity of product contained within a vessel directly affects its dynamic response. Using an ensemble of four "identical" pressure vessels as a case study, a comprehensive set of fragility curves is developed, each corresponding to a different fill ratio of a single vessel. Then, different approaches are explored to combine said fragilities and assess the group of four. These include full-scale Monte Carlo simulation with or without filling level correlation, as well as the computation of a single "law-of-total-variance" fragility curve. The latter approach is decidedly simpler, yet its use cannot be justified without some knowledge of the facility's operational profile in terms of day-to-day fluctuation of the filling level, as it can otherwise lead to unconservative and/or biased results.*

1. Introduction

Pressure vessels are structures typically encountered in oil refineries for the storage of gaseous fuels, such as propane or butane. Safety is the primary consideration for these assets, not only for ensuring the smooth operation of the facility, but also to prevent catastrophic accidents with very high environmental and financial cost. Most research studies specifically address pressure vessels from the earthquake-resistant design perspective (e.g., Moss 2004; Wieschollek et al. 2014) but also from a risk assessment perspective (e.g., Moschonas et al. 2014; Karakostas et al 2014; Öztürk et al 2021; Karaferis et al 2023). The latter relies on the reliable and accurate assessment of structural performance in case of an earthquake. This way the stakeholders would be able to safeguard the refinery's integrity and plan ahead in terms of estimating potential losses from interruptions in production or potential need for repairs, determine mitigation strategies, and formulate emergency response plans.

Regarding the seismic response of pressure vessels, one of the most critical parameters to be considered in the assessment is the fill ratio (e.g., Sezen and Whittaker 2006, Yazdanian et al. 2020a and 2020b). Whether the vessels are empty, half-empty or full directly affects their dynamic response, since it determines the convective and impulsive masses that are activated by the seismic motion. In case of an earthquake event, the fill ratio of vessels in the refinery is uncertain and practically impossible to be known a priori. This may not be a problem for design, as one will always conservatively assume a full vessel; such an assumption is not acceptable for an unbiased assessment and the resulting uncertainty in the fill ratio should be expected to propagate to the seismic response and increase its variability.

As a case study, a typical pressure vessel is examined as a case study. A reduced-order model is developed for the dynamic nonlinear analysis of the structure and high-quality fragility curves for different fill ratios are produced. Using a probabilistic approach via Monte Carlo analysis and by exploiting these partial fragilities per fill ratio, a comprehensive quantification of the fill ratio variability is achieved. Additionally, the effects of different correlation assumptions for the fill ratio are explored in a group of four identical vessels. Analytical fragility combination methods for each case are also proposed and tested against the Monte Carlo analysis results to assess their suitability for incorporating them in a risk study.

2. Model description

Spherical pressure vessels are elevated structures supported by columns, either equipped with X-bracing or not (Figure1). The examined tank consists of a 20.22 m diameter sphere that is supported by 12 columns with X-bracing; the height to the equator is equal to 13.63 m (Moschonas et al., 2014). A reduced-order numerical model (Figure 2) is developed to analyze the structure. The vessel and its containment's masses are discretized into two discrete, concentrated masses, i.e., corresponding to the impulsive and the convective mass component (Karamanos et al 2006; Patkas and Karamanos 2007; Drosos et al. 2008). The convective mass pertains to the mass of the sloshing fluid content of the vessel, while the impulsive mass typically includes the majority of the vessel's content and the mass of the shell, vibrating horizontally; both are located at the center of the sphere. The convective mass is connected to the impulsive one via translational zero-length element springs, while the latter is connected to the columns via rigid links. The columns are meshed into nonlinear beam-column elements and the braces are modelled with nonlinear truss elements. The flexibility of the spherical shell is neglected since the shell is not expected to fail before the supporting system. The welded connections of the shell to the columns are assumed to have sufficient overstrength. For more details about the modelling assumptions adopted the interested reader can refer to Karaferis et al. (2023).

The amount of content in the spherical vessel is expressed by its fill ratio. Different fill ratio cases were examined, ranging from 0.35 to 0.95 with an increment of 0.10. The variation of the fill ratio actually results in a different structure in terms of dynamic response to an earthquake excitation. As expected, spherical pressure vessels with low fill ratios are less vulnerable to earthquakes. The different properties in terms of the impulsive (T_I) and convective (T_C) eigenperiods per fill ratio are presented in Table 1 following eigenvalue analysis. It should be noted that only the first sloshing mode was accounted for, since higher modes have a very small contribution to the structure's response. A damping ratio of 2% was assumed at the impulsive mode of the vessel.

Figure 1. Illustration of a group of four spherical pressure vessels.

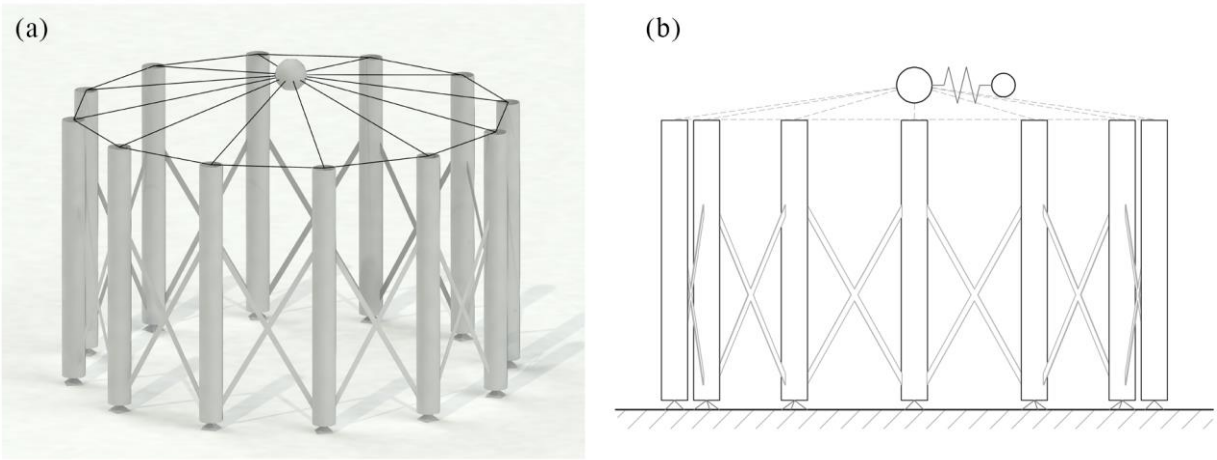

Figure 2. Schematic representation of the developed reduced-order numerical model for the spherical pressure vessel.

Table 1. Impulsive and convective eigenperiods of the pressure vessel per fill ratio.

Fill Ratio, *FR*	0.95	0.85	0.75	0.65	0.55	0.45	0.35
T_I (s)	0.65	0.59	0.53	0.47	0.41	0.37	0.33
T_C (s)	2.66	3.50	4.11	4.56	4.93	5.25	5.54

3. Fragilities

The computation of the fragility curves for the structure under investigation has followed the well-established procedure in the literature (e.g., Silva et al. 2014; Baker 2015; Bakalis and Vamvatsikos 2018). Different fragility curves were calculated for all fill ratios using Incremental Dynamic Analysis (IDA, Vamvatsikos and Cornell 2002). The horizontal displacement (D_{PV}) at the center of the spherical vessel (location of the impulsive mass) was adopted as the engineering demand parameter (EDP). D_{PV} is generally calculated as the square-root-sum-of-squares (SRSS) combination of the X and Y responses in the 3D model. The adoption of D_{PV} as the main demand indicator is a reasonable simplification since D_{PV} essentially maps one-to-one to all other EDPs, with the pressure vessel model fully conforming to the theoretical framework underlying the nonlinear static procedure. Therefore, different Damage States (DS) can be examined by tying their effects to the corresponding D_{PV}. The adopted DS classification and the corresponding capacity thresholds in terms of displacement at the center of the spherical vessel were: DS1: First yielding of any brace in tension with capacity threshold $D_{PV} = 6.30\text{cm}$, DS2: Yielding of more than 50% of braces in tension with capacity threshold $D_{PV} = 9.10\text{cm}$, and DS3: Fracture of any brace with capacity threshold $D_{PV} = 17.10\text{cm}$. For the sake of brevity, only results obtained for DS1 will be discussed henceforth.

The intensity measure (IM) adopted in the analysis is the geomean peak ground acceleration (*PGA*), which is an asset-agnostic IM that has found considerable use in portfolio-level studies. “Partial” fragility results were computed per fill ratio and are illustrated in Figure 3. As expected, a considerable variation is observed in terms of the probability of exceedance (PoE) for the considered DS1 with respect to different fill ratios. For example, for $PGA = 0.3\text{g}$ the PoE values are equal to 3.6%, 8.4%, 25.1%, 30.3%, 42.0%, 52.1% and 56.2% respectively for increasing fill ratios from 0.35 up to 0.95 (Figure 3). This variation demonstrates the effect of the fill ratio and the need for its consideration in a risk assessment study. The fragility parameters calculated for each case of fill ratio are tabulated in Table 2, employing a lognormal assumption in terms of the distribution fits.

Table 2. Pressure vessel lognormal "partial" fragility parameters per fill ratio for DS1 (first yield of any brace in tension).

Fill Ratio, *FR*	0.95	0.85	0.75	0.65	0.55	0.45	0.35
Median, *μ* (g)	0.27	0.29	0.34	0.39	0.44	0.55	0.64
Dispersion, *σ*	0.68	0.64	0.62	0.51	0.57	0.44	0.42

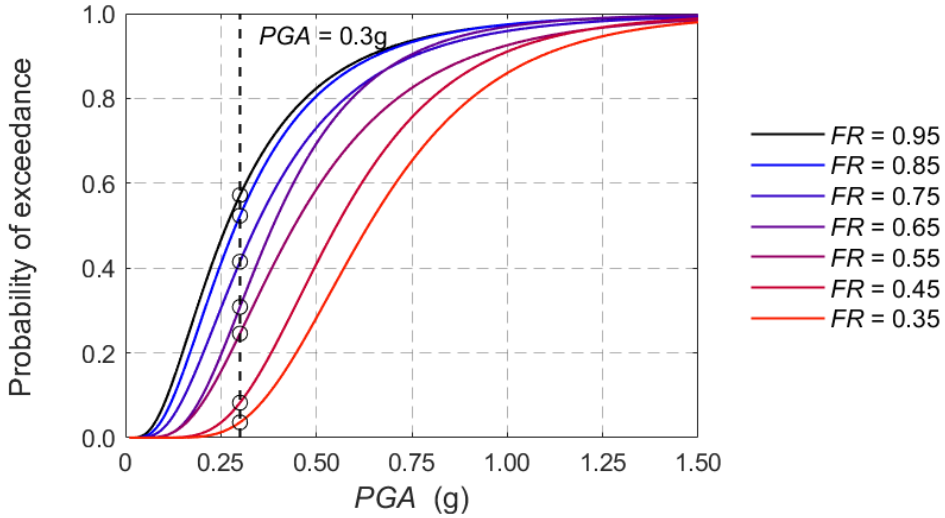

Figure 3. Pressure vessel "partial" fragilities for DS1 per fill ratio.

4. Fill ratio variability

Pressure vessels often come in groups within a refinery or storage facility (tank farm), potentially only differing in their fill ratios at any given time due to operational reasons. In general, to properly assess the performance of these vessels, their fill ratios can be numerically simulated using the partial fragility functions (see Section 3) to define the overall risk through a Monte Carlo analysis. Certainly, some knowledge of the fill ratio correlation between the different vessels is required in order to improve the reliability of the results. This information requires case-specific realistic data, which may not be available due to confidentiality reasons. Therefore, the two extreme cases of full and zero correlation between the vessels' fill ratios are adopted for quantifying the seismic risk of the group. In more detail, a group of 4 identical pressure vessels is analyzed, being located close enough (typically for safety reasons of the entire facility) and thus being subjected to the same level of seismic intensity; in other words, the spatial variability of the ground motion is insignificant. Monte Carlo simulation was employed to generate 200 realizations of the 4 pressure vessels, assigning an FR value to each. It is assumed that the failure of any vessel (attainment of the DS considered) signals the attainment of the DS for the entire group of tanks. Moreover, for the case at hand, weights of $w_i = [0.2, 0.2, 0.2, 0.1, 0.1, 0.1, 0.1]$ were assigned to the partial fragilities calculated for $FR = [0.95, 0.85, 0.75, 0.65, 0.55, 0.45, 0.35]$, meaning that the three higher FRs are assumed to be twice as likely compared to the others. Still, relevant data from the facility operator are required in a case-specific study in order to improve the accuracy of the seismic risk estimations.

At first, the case of full FR correlation is examined, meaning that all 4 vessels have the same (random) FR for all different realizations of the group. Therefore, the same PoE is obtained for all tanks for any specific realization, depending on the FR that has been randomly assigned to them. Therefore, for any given seismic event all the vessels will reach the same DS and in general reach the same level of damage at the same time. This means that for the case of full correlation, the PoE of the group coincides with the PoE of a single vessel. As an example, the results for DS1 and $PGA = 0.3\text{g}$ (obtained from Figure 3) are depicted in Figure 4. All 200 realizations of PoE are showcased depending on the vessel's fill ratio and corresponding partial fragility. Each realization is equiprobable and the 5th, 50th, and 95th percentiles are shown in Figure 4 to offer a better

understanding of the distance between higher and lower PoE values. It should be noted that since all PoE values calculated from the fragilities stem from 7 discrete values of different weights, the resolution of the percentiles' calculation ends up mapping the 5th percentile to the lowest value and the 95th percentile to the maximum of the seven. This should not be considered as problematic in general and can be overridden by employing additional intermediate FR values rather than only the seven selected.

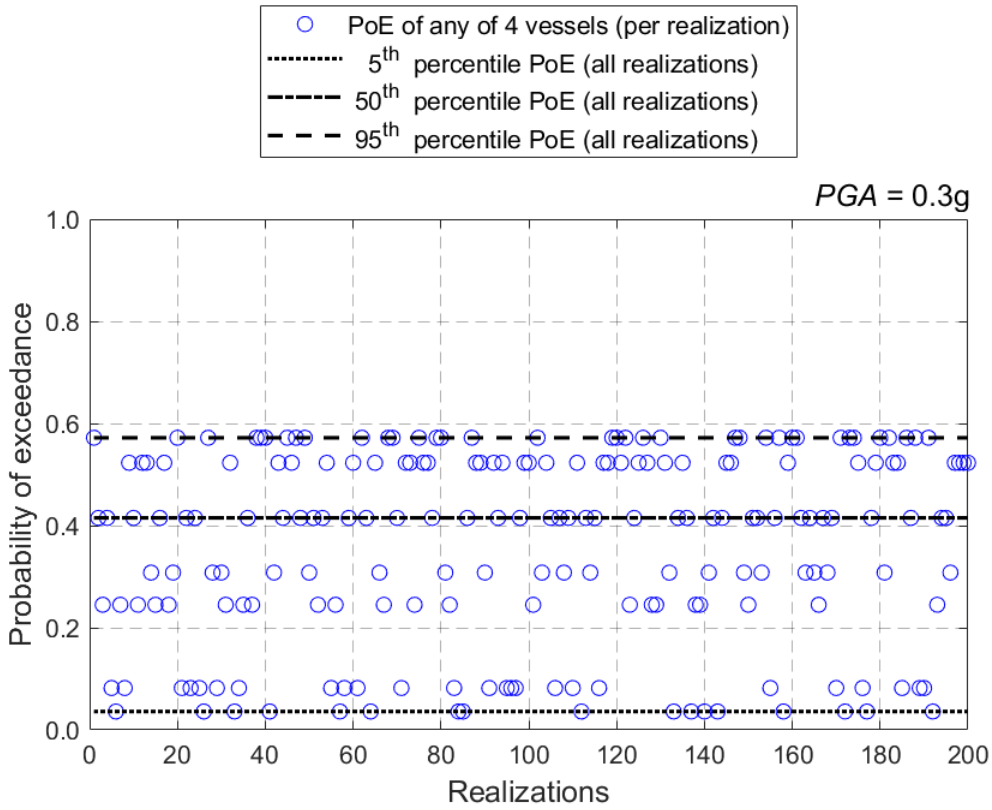

Figure 4. Monte Carlo realizations for the PoE of DS1 for the group of 4 vessels, given full FR correlation and PGA = 0.3g.

The 5th, 50th, and 95th percentile fragilities are presented in Figure 5, calculated by repeating the Monte Carlo analysis (presented before for $PGA = 0.3\text{g}$) for all IM values within the range 0.00g to 1.50g. Then, lognormal fitting is employed to derive the corresponding fragility parameters, listed in Table 3.

Table 3. Pressure vessel lognormal fragility parameters for the 5th, 50th, and 95th percentiles, assuming full FR correlation.

Percentiles	5th	50th	95th
Median, μ (g)	0.64	0.34	0.27
Dispersion, σ	0.42	0.61	0.68

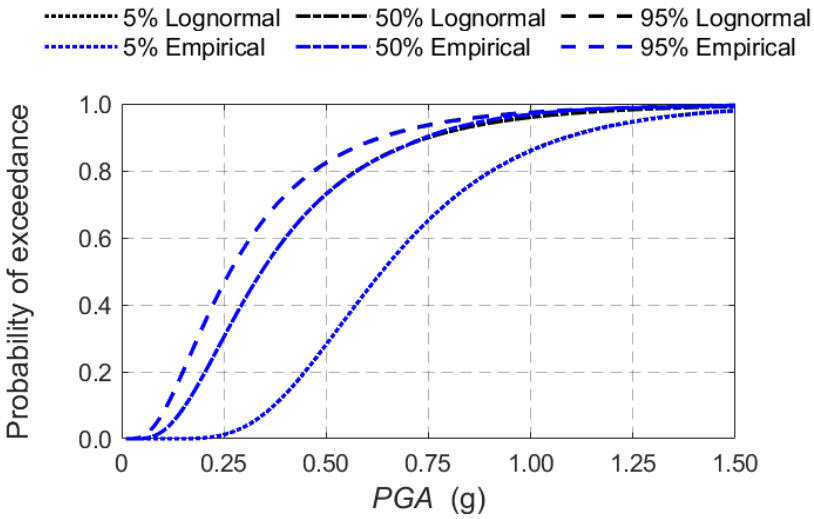

Figure 5. Pressure vessel fragilities for the 5th, 50th, and 95th percentiles, according to the results of the Monte Carlo analysis assuming full FR correlation.

The second assumption examined considers zero correlation regarding FR between the different vessels. This may be considered as a more realistic case, since each vessel can have any fill ratio per realization, therefore being characterized by a different fragility. To calculate the new uncorrelated capacity thresholds, the numerical approach employed should involve a second layer of Monte Carlo, whereby for each of the original 200 FR realizations, additional 1000 realizations of DS-exceedance were generated, based on the partial fragility's PoE. For example, say that for a single vessel of the group, considering the FR assigned to it, the PoE for DS1 is 60%. Then, in the second layer of realizations 60% of the values will signify exceedance and 40% non-exceedance, in random order. By repeating this process for the rest of the vessels, we can check for each one of the 1000 realization whether there is at least one exceedance of DS1, leading to the characterization of the entire group as reaching DS1 for the realization at hand. It is evident that doing this exercise for 1000 times on each one of the 200 realizations of the first level, the uncorrelated ensemble PoE is recalculated for the entire group with sufficient accuracy. The group PoE for each of the 200 realizations is showcased in Figure 6 indicatively for $PGA = 0.30\text{g}$. It is important to note that in all cases this PoE is higher compared to the maximum PoE of a single vessel. This signifies that given the zero-correlation assumption, simply taking the worst PoE computed for a single vessel of the group leads to the underestimation of the overall PoE. This is attributed to the lower but non-negligible probabilities of failure for the other vessels, e.g., if one vessel has 60% probability of reaching a DS and another has 40%, it is not always the case that the first one will be the one to transition to the DS in question. As considered before, the realizations in Figure 6 are equiprobable and the 5th, 50th, and 95th percentiles are presented in order.

Subsequently, the 5th, 50th, and 95th percentile fragilities are presented in Figure 7. They are calculated again by using the (double) Monte Carlo process employed for calculating the values of Figure 6, for all IM values within the range of 0.00g to 1.50g. Then, using the 5th, 50th, and 95th empirical results, a lognormal fitting is employed to produce the fragilities shown in Figure 7, while the corresponding lognormal parameters are summarized in Table 4. An important remark for the fragility curves of the group is that the median values are much lower when considering zero FR correlation, compared to the case of full FR correlation. This results from the treatment of the vessel group a series system since the failure of a single vessel would affect the functionality of the entire refinery. On the other hand, a much lower variability is observed, both in terms of the 5th, 50th, and 95th fragility dispersions and the distance between the 5th and 95th percentile fragilities in the zero-correlation case, compared to the one with full correlation.

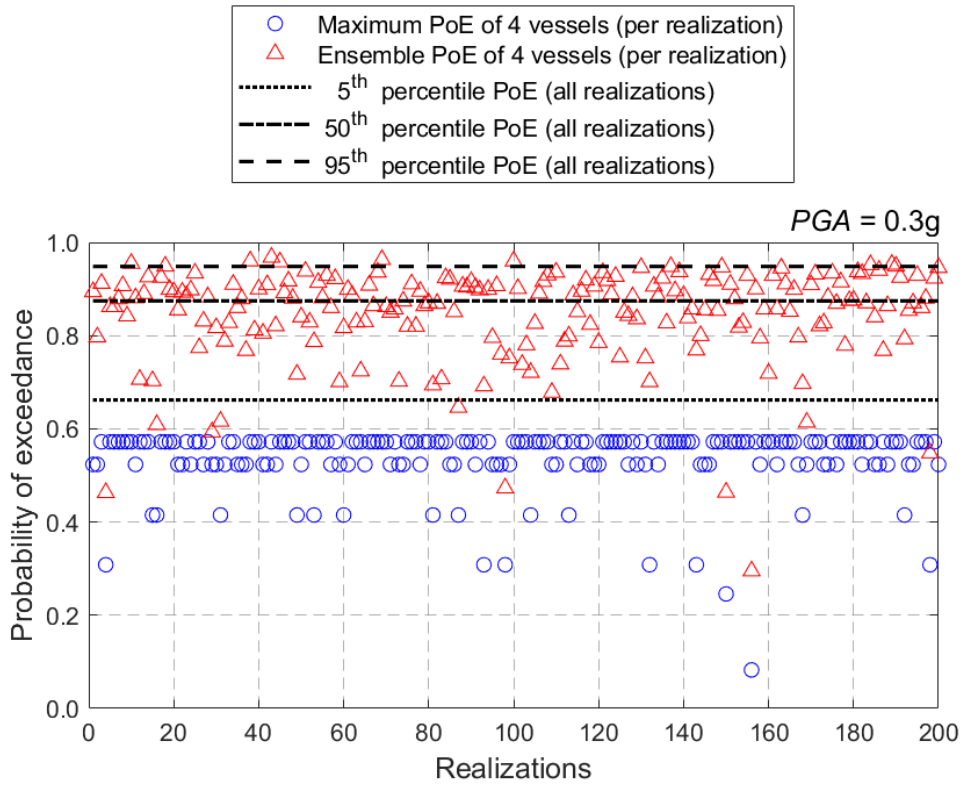

Figure 6. Monte Carlo realizations for the PoE of DS1 for the four-vessel group, given zero FR correlation and PGA = 0.3g.

Table 4. Pressure vessel lognormal fragility parameters for the 5th, 50th, and 95th percentiles based on the results of the Monte Carlo analysis, assuming zero FR correlation.

Percentiles	5th	50th	95th
Median, μ (g)	0.26	0.18	0.15
Dispersion, σ	0.44	047	0.46

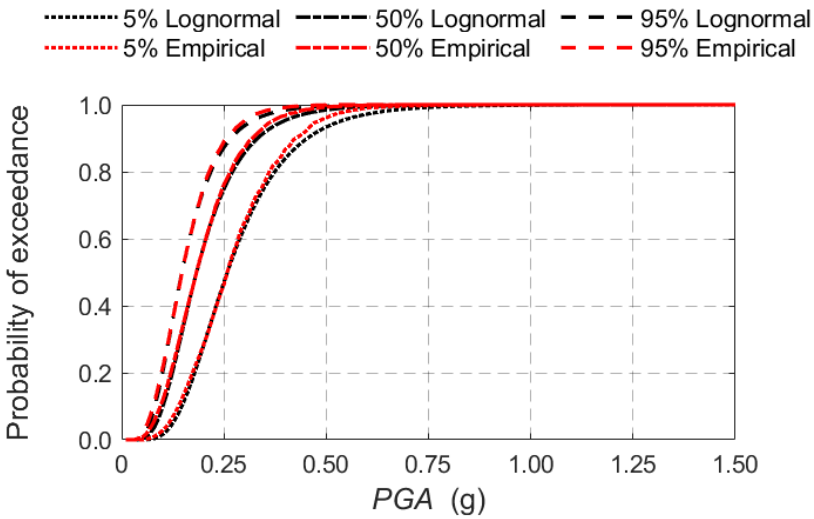

Figure 7. Pressure vessel fragilities for the 5th, 50th, and 95th percentiles, according to the results of the Monte Carlo analysis assuming zero FR correlation.

5. Fragility combination

Although the procedure presented in Section 4 can provide a sufficient representation for a group of pressure vessels, carrying out the required analysis could be cumbersome in practice. A more flexible way to calculate analytically the 50th percentile fragility of the group for both cases of FR correlation is presented hereinafter.

At first, the partial fragilities (i.e., for a single vessel) per FR for the considered DS should be combined in an overall representative combined fragility for a single structure. Given the weights of $w_i = [0.2, 0.2, 0.2, 0.1, 0.1, 0.1, 0.1]$ assigned to the partial fragilities calculated for $FR = [0.95, 0.85, 0.75, 0.65, 0.55, 0.45, 0.35]$, respectively, the law of total expectation can be employed to calculate the overall logarithmic mean using Eq (1), while the law of total variance for the overall dispersion is estimated after Eq (2) (Weiss, et al. 2005; Benjamin and Cornell 2014):

$$\ln \mu_{comb} = \sum_{i=1}^{7} w_i \ln \mu_i \tag{1}$$

$$\sigma_{comb} = \sqrt{\sum_{i=1}^{7} w_i (\sigma_i)^2 + \sum_{i=1}^{7} w_i (\ln \mu_i - \ln \mu_{comb})^2} \tag{2}$$

where μ_i and σ_i are the partial fragility medians and dispersions, while μ_{comb} and σ_{comb} are the resulting combined fragility lognormal parameters.

The combined single-vessel fragility is presented in Figure 8 together with the partial fragilities used for its calculation. It is observed that the combined fragility curve is located in the left-hand side within the range of partial fragilities, a fact attributed to the weights w_i adopted that "favor" higher FRs. For the case of full FR correlation, since all vessels are assumed to always behave in the same way, the single vessel combined fragility also characterizes the system as a whole.

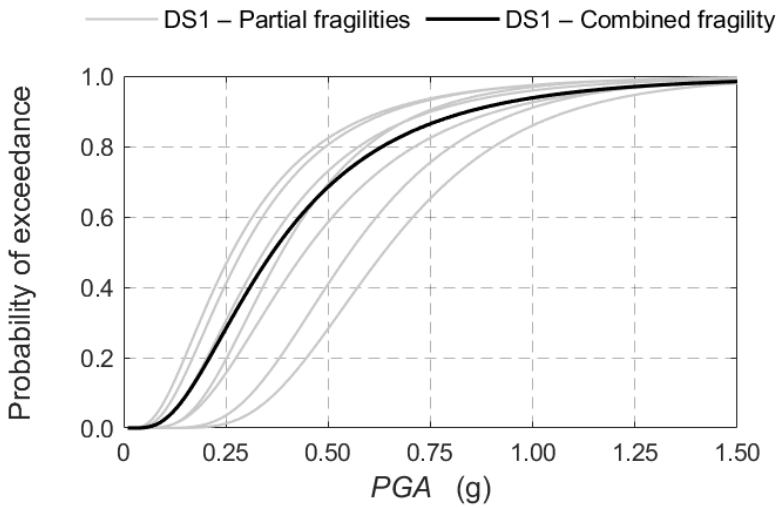

Figure 8. Partial fragility curves of a single vessel (shown with light grey lines) and combined fragility of the single vessel (shown with black line), considering the FR weights. In case of full FR correlation within the group of pressure vessels, the combined fragility of the single vessel coincides with the 50th percentile fragility of the group.

For the analytical approximation of the zero-correlation group fragility one needs to employ a logical OR combination (or union) of four identical single-vessel combined fragilities. This is typical for series systems,

and it is easily resolved by taking the inverse route, meaning that the failure of any of the four vessels is the negative of having all four vessels without failure (Benjamin and Cornell 2014):

$$P(\text{at least one vessel fails}) = 1 - P(\text{no vessel fails}) = \\ = 1 - \prod_{i=1}^{N} P(\text{vessel } i \text{ does not fail}) = 1 - (1-p)^N \quad (3)$$

where N is number of vessels with the same (single-vessel combined) fragility and p is the PoE of each individual vessel.

An important clarification should be that in Eq. (3) only point-by-point (or IM level by IM level) estimates are offered, rather than the full fragility definition like the one provided by Eqs (1) and (2) for the full correlation case. Thus, a lognormal fit is applied to the analytical assessment results of this case to calculate the parameters of the group fragilities for the DS at hand.

In Figure 9 the analytical estimations of the combined fragilities for both full and zero correlation are compared to the Monte Carlo 50th percentile fragilities. The matching is deemed satisfactory for the zero correlation case, while for the full correlation case the analytical fragility seems to slightly underestimate the Monte Carlo obtained fragility values of PoE for $IM > 0.25\text{g}$, which is acceptable because the fragilities are still quite close, considering also the simplicity of the methods applied for computing the analytical fragility curves via Eqs (1)–(3). Generally, the deviations between the analytical fragility results and the ones from the Monte Carlo simulations can be attributed either to the lognormal fitting, or to the number of Monte Carlo realizations, i.e., more than 200 realization may be required. In any case, the computed fragilities are reliable enough and a useful tool for estimating the vulnerability of a pressure vessel group, regardless of their limitations.

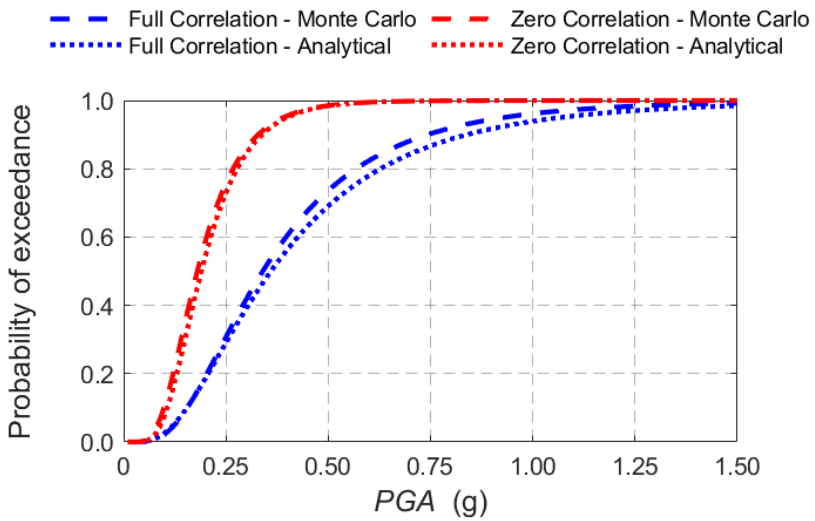

Figure 9. Analytically derived group fragilities and the corresponding Monte Carlo generated 50th percentile fragilities for both full and zero FR correlation for the four-pressure vessel system examined.

6. Conclusions

The amount of product stored in spherical pressure vessels, as expressed by the fill ratio (FR), is a critical parameter that determines the dynamic response of the vessel and has to be considered explicitly in a seismic risk assessment study. Therefore, employing fill-ratio-dependent "partial" fragilities should be the appropriate approach. Still, explicitly employing fill-ratio-dependent fragilities within a risk analysis may be an onerous requirement. Instead, when examining a single vessel, a "combined" fragility curve can be derived from the partial ones (for different fill ratios), by accounting for the likelihood of the fill ratios. When a group of vessels is examined, the correlation of the fill ratios among the vessels in the group also comes into play. If a single representative "group" fragility is sought in the general case of partial correlation, Monte Carlo simulation is

required to combine the partials. In the two boundary cases of full and zero FR correlation, analytical approximations are also possible. For full correlation, the group fragility coincides with the single vessel combined fragility; for zero correlation, a simple series system assumption can be employed to painlessly determine the group fragility. In all cases, the zero correlation assumption by far leads to more severe results, showcasing the need for realistic operational data on quantities usually stored in the vessels to allow a more favorable non-zero-correlation outcome.

7. Acknowledgements

Financial support has been provided by the Hellenic Foundation for Research and Innovation (H.F.R.I.) under the “2nd Call for H.F.R.I. Research Projects to support Faculty Members & Researchers”, Project “TwinCity: Climate-Aware Risk and Resilience Assessment of Urban Areas under Multiple Environmental Stressors via MultiTiered Digital City Twinning” (Grant Agreement 2515) and by the European Framework Programme for Research and Innovation (Horizon 2020) under the “YADES” Marie Skłodowska-Curie project with Grant Agreement No 872931.

8. References

Bakalis, K., Vamvatsikos, D. (2018) Seismic fragility functions via nonlinear response history analysis. *J. Struct. Eng. (ASCE) 144(10), 04018181*. https://doi.org/10.1061/(ASCE)ST.1943-541X.0002141

Baker, J.W. (2015). Efficient analytical fragility function fitting using dynamic structural analysis. *Earthq. Spectra 31(1), 579–599*. https://doi.org/10.1193/021113EQS025M

Benjamin, J.R., Cornell, C.A. (2014) *Probability, Statistics, and Decision for Civil Engineers*. Dover Publications, Mineola NY

Drosos, G.C., Dimas, A.A., Karabalis, D.L. (2008). Discrete models for seismic analysis of liquid storage tanks of arbitrary shape and fill height. *ASME J. Press. Vessel Technol*. https://doi.org/10.1115/1.2967834

Karakostas, C. Z., Moschonas, I. F., Lekidis, V. A., Papadopoulos, S. P. (2015). Seismic performance of industrial pressure vessels: Parametric investigation of simplified modeling approaches for vulnerability assessment. *Proceedings of 5th International Conference on Computational Methods in Structural Dynamics and Earthquake Engineering (COMPDYN 2015), pp. 2021–2037. Crete Island, Greece.*

Karamanos, S.A., Patkas, L.A., Platyrrachos, M.A. (2006). Sloshing effects on the seismic design of horizontal-cylindrical and spherical industrial vessels. *ASME J. Press. Vessel Technol. 128(3), 328–340.* https://doi.org/10.1115/1.2217965

Moschonas, I., Karakostas, C., Lekidis, V., Papadopoulos, S. (2014). Investigation of seismic vulnerability of industrial pressure vessels. *Second European Conference on Earthquake Engineering and Seismology (2ECEES), pp. 25–29. Istanbul August.*

Moss, D.R. (2004). *Pressure Vessel Design Manual: Illustrated Procedures for Solving Major Pressure Vessel Design Problems*, 3rd ed. Gulf Professional Publishing Elsevier, London https://doi.org/10.1016/B978-0-7506-7740-0.X5000-8

Öztürk, S., Akgül, K., Sari, A. (2021). Seismic fragility and behavior of spherical pressure vessels. *Pressure Vessels and Piping Conference, Vol. 85352, p. V005T08A019. American Society of Mechanical Engineers.* https://doi.org/10.1115/PVP2021-61069

Patkas, L.A., Karamanos, S.A. (2007). Variational solutions for externally induced sloshing in horizontal-cylindrical and spherical vessels. *ASCE J. Eng. Mech. 133(6), 641–655.* https://doi.org/10.1061/(ASCE)0733-9399(2007)133:6(641)

Sezen, H., Whittaker, A.S. (2006). Seismic performance of industrial facilities affected by the 1999 Turkey earthquake. *ASCE J. Perform. Constr. Facil. 20(1), 28–36.* https://doi.org/10.1061/(ASCE)0887-3828(2006)20:1(28)

Silva, V., Crowley, H., Varum, H., Pinho, R., Sousa, R. (2014). Evaluation of analytical methodologies used to derive vulnerability functions. *Earthq. Eng. Struct. Dyn. 43(2), 181–204.* https://doi.org/10.1002/eqe.2337

Vamvatsikos, D., Cornell, C.A. (2002). Incremental dynamic analysis. *Earthq. Eng. Struct. Dynam. 31(3), 491–514.* https://doi.org/10.1002/eqe.141

Weiss, N.A., et al. (2005) *A Course in Probability*. Pearson Addison Wesley, Boston

Wieschollek, M., Pinkawa, M., Hoffmeister, B., Feldmann, M. (2014). Seismic design of spherical pressure vessels. *Seismic Design of Industrial Facilities: Proceedings of the International Conference on Seismic Design of Industrial Facilities (SeDIFConference), pp. 417–428. Springer Fachmedien Wiesbaden* https://doi.org/10.1007/978-3-658-02810-7_35

Yazdanian, M., Ingham, J.M., Kahanek, C., Dizhur, D. (2020a). Damage to flat-based wine storage tanks in the 2013 and 2016 New Zealand earthquakes. *J. Constr. Steel Res. 168, 105983.* https://doi.org/10.1016/j.jcsr.2020.105983

Yazdanian, M., Ingham, J.M., Kahanek, C., Dizhur, D. (2020b). Damage to legged wine storage tanks during the 2013 and 2016 New Zealand earthquakes. *J. Constr. Steel Res. 172, 106226.* https://doi.org/10.1016/j.jcsr.2020.106226